

Intruder state collectivity at a double subshell closure from the beta decay of 0^- $^{96}\text{Y}^g$ to the levels of ^{96}Zr

H. Mach

Clark University, Worcester, Massachusetts 01610;
Brookhaven National Laboratory, Upton, New York 11973;
University of Maryland, College Park, Maryland 20742

G. Molnár* and S. W. Yates

University of Kentucky, Lexington, Kentucky 40506

R. L. Gill

Brookhaven National Laboratory, Upton, New York 11973

A. Aprahamian[†]

Clark University, Worcester, Massachusetts 01610

R. A. Meyer

Lawrence Livermore National Laboratory, Livermore, California 94550

(Received 20 May 1987)

Levels of ^{96}Zr populated following the β^- decay of the 0^- ground state of ^{96}Y have been investigated by γ -ray and conversion electron singles, γ -ray multispectral scaling, γ - γ and γ - e^- coincidence, and γ - γ angular correlation measurements. These data have been used to establish the population of eight excited levels of ^{96}Zr , to confirm the 0^+ assignment of the 2695-keV level, and to determine a half-life of 5.4(1) s for ^{96}Y . The deduced beta transition strengths establish the decay to the ground state, with $\log ft$ of 5.6, as one of the fastest first-forbidden decays known and support the notion of double subshell closure at $Z=40$ and $N=56$. The observed strong hindrance of transitions to excited 0^+ states is indicative of shape coexistence. The observed level pattern of the band built on the 0_2^+ state exhibits similarities to nearby vibrational-like nuclei having four valence protons and four valence neutrons. A four-particle, four-hole interpretation of the 0_2^+ state is supported by the data, and we determine a deformation parameter, $\beta_2 \sim 0.2$, for this intruder bandhead.

I. INTRODUCTION

The nucleus of ^{96}Zr has several unusual features. One such feature is its nearly magic character resulting from the double subshell closure at $Z=40$ and $N=56$ as shown by the energy of the first excited 2^+ state¹ at 1750 keV and the purity of the ground state configuration.² Also, the lowest excitation is a 0^+ state, which exhibits unusually strong excitation in the two-neutron stripping³ and alpha-pickup reactions.⁴ This state and two associated levels with spin 2^+ and 4^+ were recently identified⁵ as members of an intruder band and were interpreted as four-particle, four-hole (4p-4h) excitations. A recent study⁶ of neighboring ^{98}Zr also demonstrated that the first excited 2^+ state associated with the ground state (g.s.) is at 1590 keV, relatively close in energy to the 1750-keV first excited 2^+ state in ^{96}Zr . This observation led to the suggestion that, for the Zr nuclei, a unique situation of double subshell closure occurs over a pair of nuclei. Evidence for the extent of the double subshell closure also comes from the characterization⁷ of a high-spin three quasiparticle state in the ^{97}Y nucleus which is, in a sense, between ^{96}Zr and ^{98}Zr . Thus, in order to

characterize better the nature of the excited states in these nuclei with doubly closed subshells, we have studied the beta decay of $^{96}\text{Y}^g$ which has been shown^{8,9} to have a spin-parity value of 0^- with predominantly a $\pi(2p_{1/2})\nu(3s_{1/2})$ g.s. configuration. We use our measured beta-transition strength to the intruder bandhead and ground state, in combination with the measured 0^+ (intruder) to 0^+ (g.s.) monopole strengths, to determine the extent of deformation of the intruder bandhead. Preliminary results of this work, together with some inelastic neutron scattering (INS) data, have already been published.^{5,10}

Prior to the present study only the g.s. and the first excited 0^+ levels in ^{96}Zr were known¹ to be populated from the beta decay of $^{96}\text{Y}^g$. Moreover, recent studies of ^{96}Zr using in-beam spectroscopic techniques¹¹⁻¹³ have led to the establishment of a number of new levels.

II. EXPERIMENTAL PROCEDURES

The measurements were performed at the online mass separator TRISTAN at Brookhaven National Laboratory. The activity was produced by thermal neutron induced fission of an enriched ^{235}U target inside the

separator's positive surface ionization (PSI) source¹⁴ which has a high efficiency for the production of ^{96}Rb and considerably lower efficiencies for ^{96}Sr and ^{96}Y . This selectivity allowed the desired low-spin isomer of ^{96}Y to be populated predominantly via the decay chain: $^{96}\text{Rb}(t_{1/2}=0.2\text{ s})\rightarrow^{96}\text{Sr}(t_{1/2}=1\text{ s})\rightarrow^{96}\text{Y}(t_{1/2}=6\text{ s})\rightarrow^{96}\text{Zr}$. The ^{96}Rb was ionized by the PSI source, extracted to form an ion beam, mass separated by a 90° magnet and deposited onto a movable, aluminized Mylar tape. The counting cycle consisted of three consecutive time intervals, T_1 , T_2 , and T_3 . The source was accumulated for a period of time, T_1 , selected to optimize the yield of the yttrium activity. At the end of T_1 , the beam was electrostatically deflected for a time interval, T_2 , to allow the short-lived ^{96}Rb and ^{96}Sr to decay. Finally, the ^{96}Y source was moved to a daughter-port counting station where various detectors were positioned to study the emitted radiations over a period of time, T_3 , after which the cycle was repeated. Typical cycle times of $T_1=10\text{ s}$, $T_2=4\text{ s}$, and $T_3=16\text{ s}$ were used for the singles, γ -ray multispectral scaling (GMS), and conversion electron studies. A different set was used for the γ - γ coincidence experiment ($T_1=T_2=T_3=6\text{ s}$), as well as for the γ - $\gamma(\theta)$ angular correlation measurements ($T_1=6\text{ s}$, $T_2=8\text{ s}$, and $T_3=6\text{ s}$).

A. Gamma-ray measurements

The gamma-ray measurements consisted of singles, GMS, γ - γ - t coincidences, γ - $\gamma(\theta)$ angular correlation measurements, and a saturation beam measurement. The saturation beam measurement is discussed in Sec. II C.

A typical γ -ray spectrum is presented in Fig. 1. The strongest γ lines arise from a strong β -delayed neutron branch of ^{96}Rb via the following decay chain: $^{96}\text{Rb}(t_{1/2}=0.2\text{ s})\rightarrow^{95}\text{Sr}(t_{1/2}=25\text{ s})\rightarrow^{95}\text{Y}(t_{1/2}=10.3\text{ min})\rightarrow^{95}\text{Zr}(t_{1/2}=64\text{ d})$. The energies of new transitions were determined from a combination of offline calibrations and internal calibrations using known¹ transitions in ^{96}Y and ^{96}Zr . The efficiency calibrations were performed offline using standard sources.

Gamma-ray transitions were assigned to the decay of ^{96}Y from the multispectral scaling measurements. In the GMS cycle time of 16 s, 32 consecutive spectra were collected. The decay curve for each transition was fitted to a single-component decay after correcting for dead time effects by normalizing to a long-lived impurity line. The decay curves for some selected transitions are illustrated in Fig. 2. The 122-keV transition from the $^{96}\text{Sr}\rightarrow^{96}\text{Y}$ decay served as an internal test of the normalization procedure. The half-life of 1.04(1) s which we determine for this line compares well with the adopted¹ value of 1.06(3) s. The half-life for the $^{96}\text{Y}^g$ decay is found to be 5.4(1) s. The statistics obtained in the experiment are sufficient to rule out any significant contribution to our data from the high-spin 10 s isomer.¹⁵ The energies, intensities, and GMS results for the transitions associated with the decay of the 0^- isomer of ^{96}Y are presented in Table I. Some of the low-intensity transitions were assigned to the decay of ^{96}Y on the basis of coincidence relations rather than the GMS results.

In the γ - γ - t measurements about 1.6×10^7 coincidence events, energies of the two transitions and the time delay between them, were stored on magnetic tapes and sorted

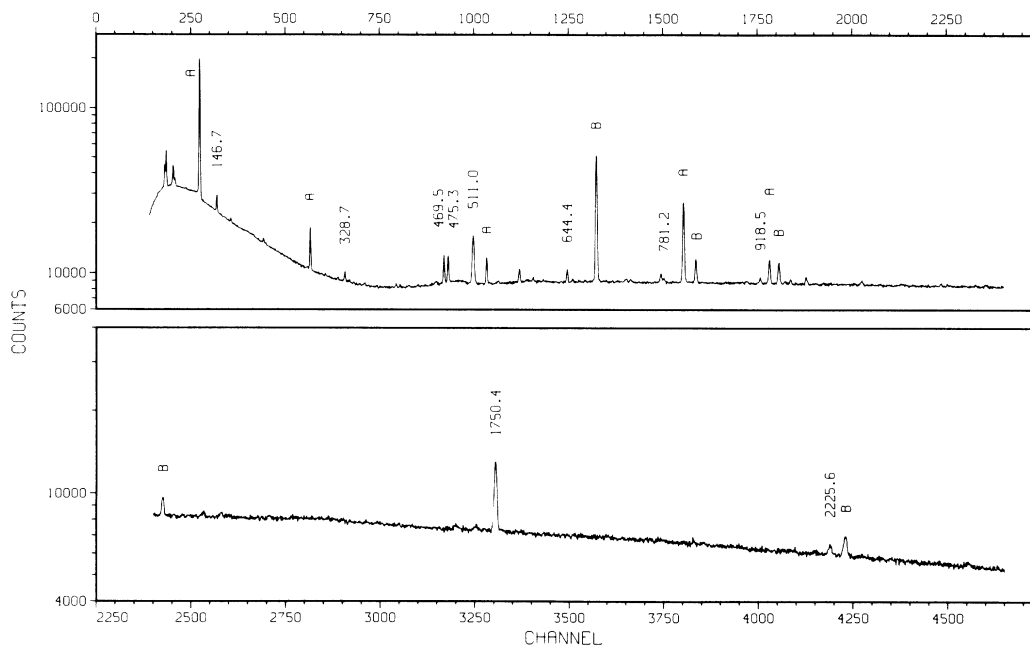


FIG. 1. A γ -ray singles spectrum with energies given for transitions in ^{96}Zr populated from the decay of the 5.4 s 0^- ground state of ^{96}Y . Dominating impurity lines from the decay of $^{96}\text{Sr}\rightarrow^{96}\text{Y}$ (A) and from the decay of $^{95}\text{Sr}\rightarrow^{95}\text{Y}$ (B) are illustrated in the figure.

offline. Figure 3 shows the spectra obtained in coincidence with the most abundant 1750- and 2225-keV transitions, respectively. Examination of the 1750-keV gamma-ray coincidence gate indicates that any missing gamma-ray intensity populating the 1750-keV level is probably less than 0.2% of all decay. A similar result comes from an analysis of the 2225-keV gate.

The γ -angular correlation experiments were performed at the daughter port using a four-detector system.¹⁶ The four detectors were positioned at distances of ≈ 7 cm from the source in a geometry which allows simultaneous measurements at six angles: 90°, 105°, 120°, 135°, 150°, and 165°. Relative detector efficiencies were obtained for each detector from a singles spectrum gated

by its own timing signal. These spectra were simultaneously accumulated during the measurement. Finite solid-angle corrections were obtained from tabulated¹⁷ attenuation coefficients. The high counting rate required for the measurement resulted in dead time effects which were different for each coincidence channel. Consequently, normalization factors were obtained from the known¹⁸ correlations in ¹⁴²Ba, which were measured under similar experimental conditions. In order to minimize any systematic errors, two cascades were selected in ¹⁴²Ba, one of positive and one of negative a_2 coefficient. Nevertheless, some residual corrections specific to the ⁹⁶Y decay are possibly unaccounted for. Inasmuch as these corrections are expected to be of the

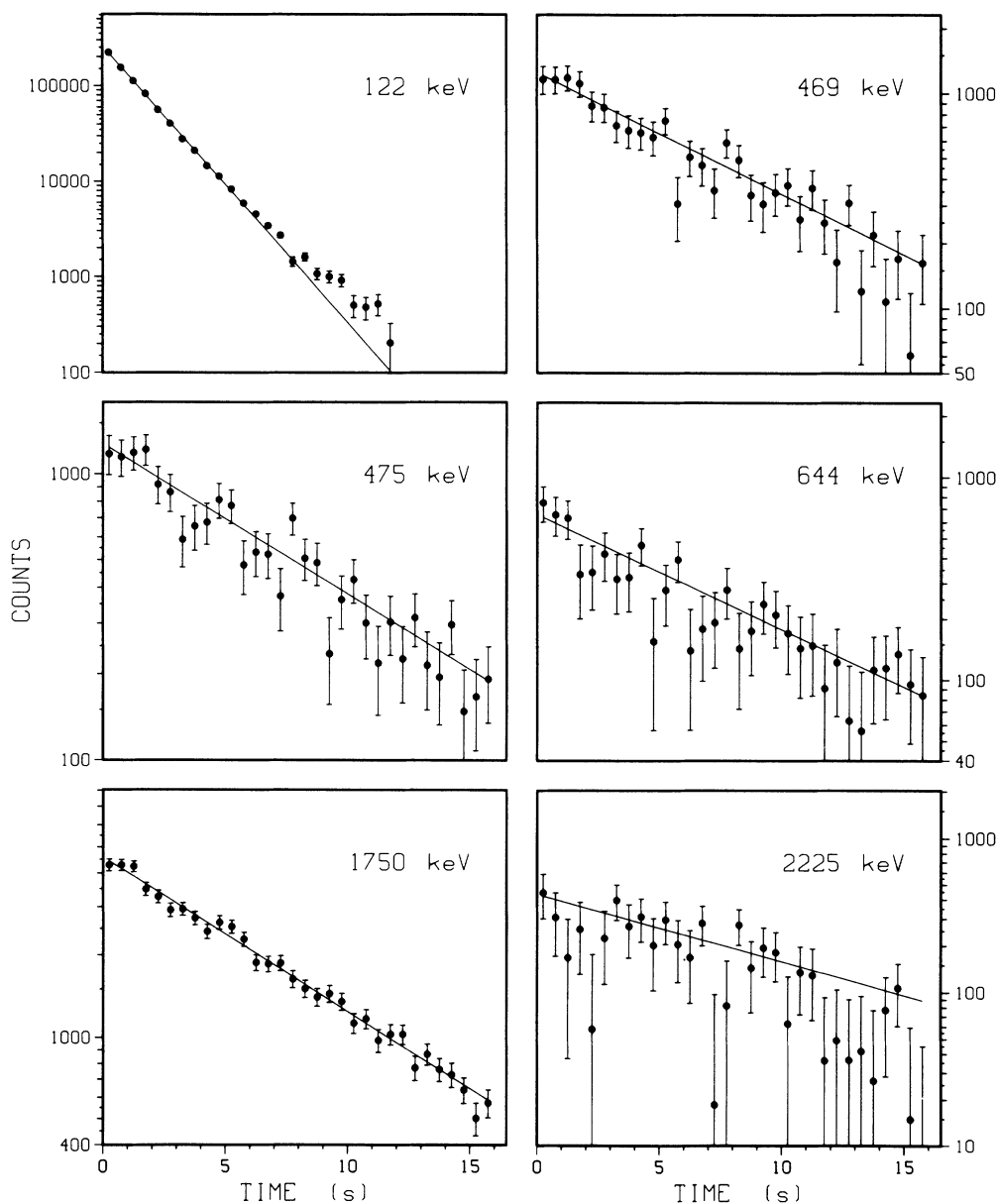


FIG. 2. Decay curves observed in the γ -ray multispectrum scaling measurement for the 122-keV photopeak in the ⁹⁶Sr decay spectrum [$T_{1/2}=1.04(1)$ s] and for the 469, 475, 644, 1750, and 2225 keV photopeaks in the decay of 5.4-s ⁹⁶Y^z. The $T_{1/2}$ values measured for the latter transitions are listed in the fourth column of Table I.

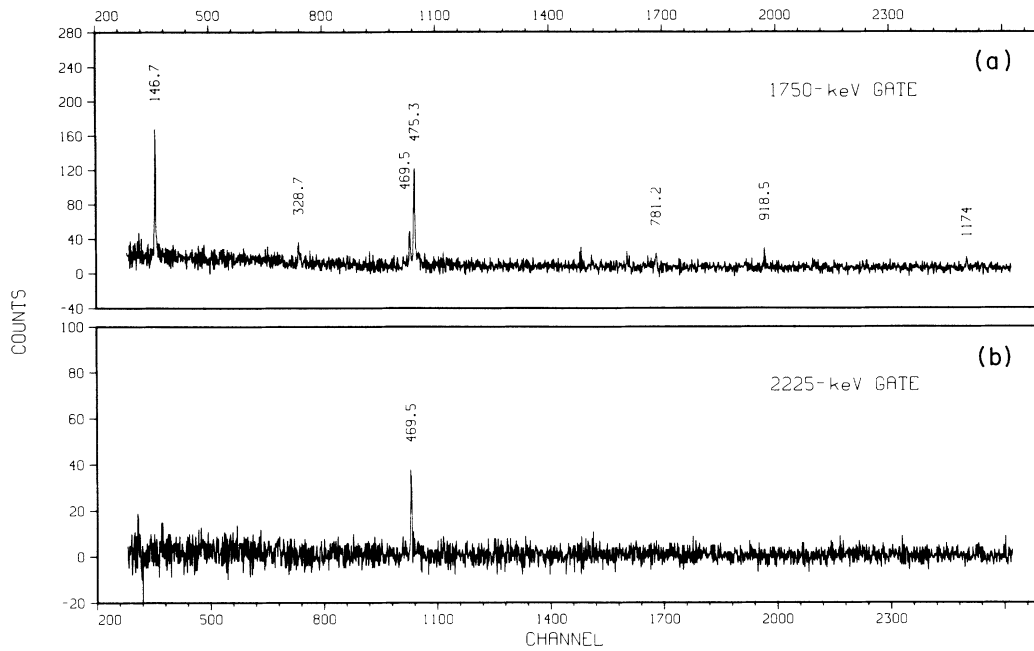


FIG. 3. Gamma-ray spectra in coincidence with (a) the 1750-keV $2_1^+ \rightarrow 0_1^+$, and (b) the 2225-keV $2_2^+ \rightarrow 0_1^+$ transitions.

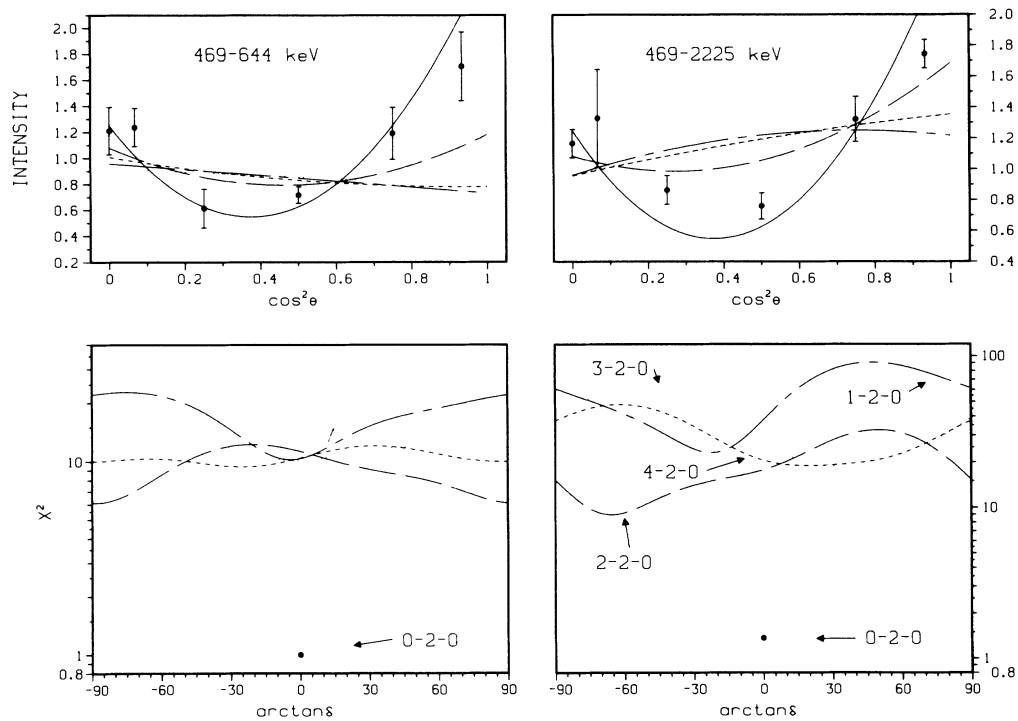


FIG. 4. Angular correlations for two cascades in ^{96}Zr : 469–644 keV and 469–2225 keV. The upper panels indicate the fit of the experimental data to the theoretical angular correlation coefficients which, for the purpose of comparison, were attenuated by the Q_2 and Q_4 coefficients. The solid line indicates the fit to the 0-2-0 sequence. In the bottom panels χ^2 is plotted against $\delta(L+1/L)$ (the latter compressed by the $\arctan \delta$ function) for a sequence of spins. Same type of lines are used in both panels to mark the same spin sequences.

TABLE I. Energies and intensities of $^{96}\text{Y} \rightarrow ^{96}\text{Zr}$ decay lines.

E_γ (keV)	I_γ^a	$E_i \rightarrow E_f$ (keV)	$t_{1/2}$ (s)
146.653(10) ^b	32(3)	1897.1 → 1750.4	5.7(3)
328.7(2)	21(2)	2225.7 → 1897.1	7.5(14)
469.5(2)	72(4)	2695.4 → 2225.7	5.3(4)
475.3(2) ^b	87(4)	2225.7 → 1750.4	5.7(4)
644.4(2)	35(2)	2225.7 → 1581.4	5.3(6)
699.4(4)	18(3)	2925.2 → 2225.7	
771.7(2)	9.1(5)	2668.9 → 1897.1	
781.2(2)	24(1)	3450.1 → 2668.9	
918.5(2)	35(2)	2668.9 → 1750.4	7.7(17)
1174.9(4)	20(4)	2925.2 → 1750.4	
1750.4(2) ^b	1000(50)	1750.4 → 0.0	5.31(12)
1897.4(3) ^b	< 5	1897.1 → 0.0	
2225.6(4) ^b	150(15)	2225.7 → 0.0	6.9(15)

E_{E0} (keV)	I_{E0}^a	$E_i \rightarrow E_f$ (keV)
1581.4(5)	480(100)	1581.4 → 0.0

^aMultiply by 0.0029(9) to obtain I_γ per 100 decays of ^{96}Y .

^b E_γ from Ref. 1.

order of a few percent in the intensities and randomly distributed among the individual angles, they would not affect the conclusions drawn from the results. The angular correlation data were fitted to the expression

$$W(\theta) = N_0 [1 + a_2 Q_2 P_2(\cos\theta) + a_4 Q_4 P_4(\cos\theta)], \quad (1)$$

where N_0 is a normalization constant, while Q_2 and Q_4 are the attenuation coefficients.¹⁷ The numerical results, together with the multipole mixing ratios obtained from a χ^2 fit of the data to the theoretical coefficients, are summarized in Table II.

Figure 4 illustrates the angular correlations for the 469–2225 keV and the 469–644 keV cascades. Both de-excite the 2695 keV level in ^{96}Zr and have angular correlations characteristic of a $0 \rightarrow 2 \rightarrow 0$ sequence. In the upper panels we have shown the theoretical angular correlations for the $0 \rightarrow 2 \rightarrow 0$ sequence (the solid lines) and for other spin sequences (indicated by broken lines). The latter were obtained from a χ^2 search against the $\delta(L+1/L)$ mixing ratio for the two lowest multiplicities that were allowed by a given spin sequence. Clearly, the $0 \rightarrow 2 \rightarrow 0$ sequence is associated with the best χ^2 , although the $2 \rightarrow 2 \rightarrow 0$ solution is also allowed by the one

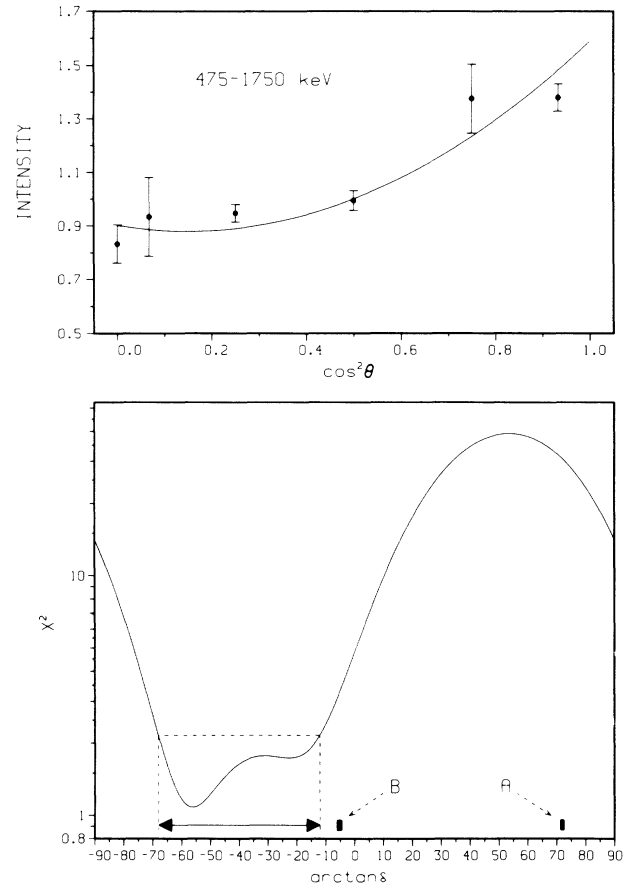


FIG. 5. Angular correlation for the 475–1750 keV cascade is presented in the top panel. The solid line indicates the correlation for the spin sequence $2 \rightarrow 2 \rightarrow 0$ and the mixing ratio for the 475-keV transition of $\delta = -1.5$ ($\arctan\delta = -56$). This parameter was found from the χ^2 fit to the theoretical coefficients as illustrated in the bottom panel. *A* and *B* represent two acceptable δ mixing ratios for the 475-keV transition obtained in the angular distribution ($n, n'\gamma$) measurement (Ref. 11).

percent χ^2 confidence limits. The latter spin sequence, however, must be rejected on the basis of excitation functions obtained in the ($n, n'\gamma$) studies.¹⁰

In Fig. 5 we show the results for the 475–1750 keV cascade which depopulates the 2_2^+ state at 2225 keV. The solid line represents the best fit to the theoretical coefficients obtained at $\delta = -1.5$ from a χ^2 search

TABLE II. Angular correlation a_2 , a_4 , and δ parameters.

Transition (keV)	a_2^{exp}	a_4^{exp}	Spin sequence	a_2^{th}	a_4^{th}	$\delta(E2/M1)$
469–644	0.13(14)	1.19(19)	$0 \rightarrow 2 \rightarrow 0$	0.357	1.143	
469–2225	0.24(9)	0.96(13)	$0 \rightarrow 2 \rightarrow 0$	0.357	1.143	
475–1750	0.36(6)	0.19(8)	$2 \rightarrow 2 \rightarrow 0$	0.365 ^a	0.224	$-1.5_{-1.0}^{+1.3}$

^a a_2 , a_4 , δ parameters from a χ^2 fit to the data obtained at the value of χ^2_{min} .

against δ for the spin sequence $2 \rightarrow 2 \rightarrow 0$. The results of this search are illustrated in the bottom panel where the δ parameter is compressed by the arctan function. The search yields a range of acceptable δ values, $\delta = -1.5^{+1.3}_{-1.0}$ (indicated on the plot by a double arrow), which satisfy the condition¹⁹ of $\chi^2 \leq \chi^2_{\min} + 1$. This value must be compared to precise angular distribution results obtained in the $(n, n'\gamma)$ experiment at Kentucky.¹¹ The latter provided two acceptable solutions, marked as *A* and *B*, which are illustrated in the bottom panel of Fig. 5. One of those solutions, *A*, $\delta = 3.07^{+0.09}_{-0.12}$, would require a negative a_2 and a large positive a_4 angular correlation coefficient ($a_2 = -0.260$ and $a_4 = 0.295$), and thus is incompatible with the present data. However, the other pair of values, $a_2 = 0.311$ and $a_4 = 0.002$, associated with the second solution, $\delta = -0.09^{+0.012}_{-0.017}$, is consistent with the results of the angular correlation measurements. In view of these facts, we adopt the latter solution.

B. Conversion electron measurements

Conversion electrons were detected in a daughter port configuration using a specialized chamber, which allowed simultaneous measurements of e^- and γ -ray singles spectra and e^- - γ coincidences; all were gated by coincident signals from a thin plastic beta detector. Approximately 5×10^5 e^- - γ -t coincident triplets were recorded. Conversion electron spectra were measured with a 200 mm² Si(Li) detector which has a 3 mm depletion depth and a full width at half maximum resolution of 1.6 keV at 624 keV. The Si(Li) energy and efficiency calibrations for conversion electrons and low-energy γ rays were measured offline using thin radioactive sources.

The beta-gated e^- spectrum is illustrated in Fig. 6. We observe strong *K* and *L* electron lines and the γ peak for the 122 keV ^{96}Y transition and dominant *K* and *L* peaks for the $0_2^+ \rightarrow 0_1^+$ *E0* transition in ^{96}Zr . We determine an energy of 1563.3(5) keV for the *E0* *K* conversion line. This results in the energy of 1581.4(5) for the g.s. *E0* transition, which is in agreement with the recent value of 1582(2) keV reported by van Klinken *et al.*²⁰ but is substantially lower than the earlier result of 1594(1) keV.^{1,21} A further confirmation of the 1581-keV value comes from the Grenoble online isotope separator data that has been recently recalibrated internally.²² This recalibration gave an *E0* transition energy of 1581.5(8) keV. In the present work this energy was also independently obtained from the coincidence requirements of the decay scheme and the γ -ray energy balances to yield a value of 1581.5(3) keV.

We have deduced the ratio of intensities between the *E0* transition and the γ -rays in ^{96}Zr from our simultaneous measurement of the β -gated e^- singles spectrum presented in Fig. 6 and a β -gated γ -ray spectrum accumulated using a Ge(Li) detector. The three peaks from the 122-keV ^{96}Y transition in the e^- spectrum and a corresponding peak in the γ -ray spectrum were used to normalize both spectra. The largest contribution to the uncertainty in the measurement arises from the uncertainties in the relative efficiencies in each detector. The intensity of the *E0* transition has been found to be 480(100) on the scale of 1000 for the 1750-keV γ ray. Figure 7 illustrates the γ -ray spectrum observed in coincidence with the 1581-keV *E0* transition. It shows only the 644.4-keV γ ray, which can be unambiguously assigned as a transition between the 2_2^+ and 0_2^+ levels. A similar assignment was recently made by Henry *et al.*¹² using in-beam $(t, p\gamma e^-)$ spectroscopy.

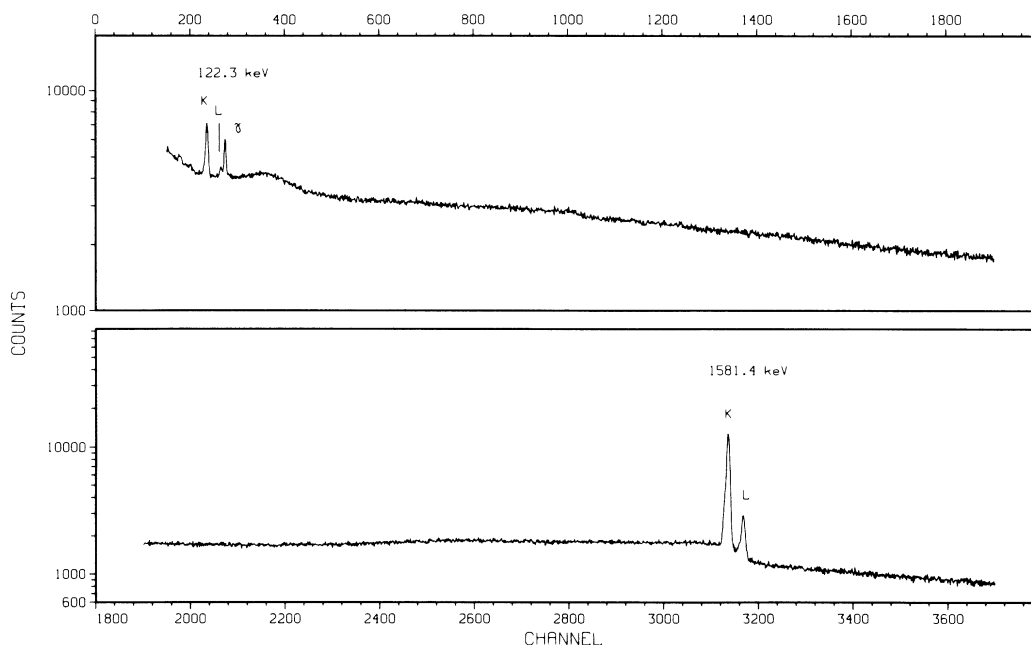


FIG. 6. Beta-gated e^- spectrum obtained with a Si(Li) detector. The *K*, *L*, and γ peaks from the 122-keV transition in ^{96}Y and the *K* and *L* peaks from the 1581-keV *E0* transition between the 0_2^+ and 0_1^+ states in ^{96}Zr are indicated in the figure.

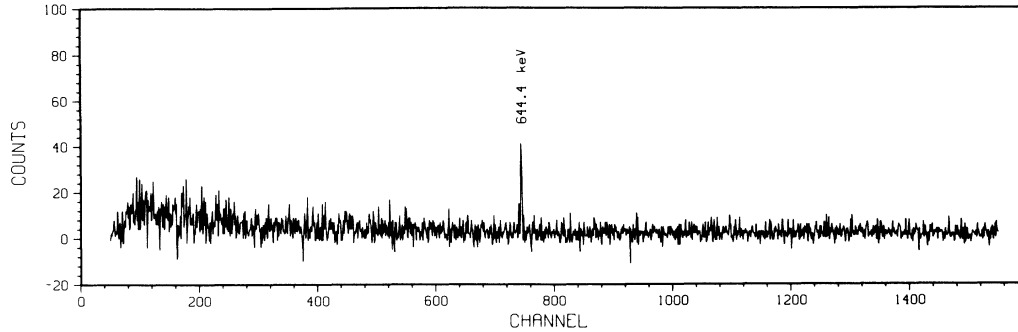


FIG. 7. Spectrum of γ -rays in coincidence with the 1581-keV $E0$ transition in ^{96}Zr . Only one photopeak at 644-keV was identified in the spectrum.

C. Saturated beam measurement

Previous studies^{1,15} have reported an absolute β feeding to the 0^+ ground state varying from 75% to 95%, with the remaining intensity ascribed to feeding of the 0_2^+ level. In order to establish the absolute beta feeding, a γ -ray singles spectrum was measured at the point of beam deposition where the source was continuously accumulated for a few hours. Using these γ -ray intensities, we have derived the absolute β^- feeding to the 0^+ ground state of ^{96}Zr from the assumption of an equilibrium among the decays in the isobaric chain. In the first step, the rates for the ^{96}Sr and ^{96}Y decays were found equal to within 12%. This value was established using the 815-keV transition in ^{96}Sr and the 122- and the 809-keV transitions in ^{96}Y , which were corrected for the absolute γ -ray branchings¹ of 76(2), 76.5(12), and 72(3) percent, respectively. This confirmed that, as expected, the PSI source gave direct production of ^{96}Sr at least an order of magnitude lower than for ^{96}Rb . In the second step, we assumed an equal source strength between the ^{96}Sr to ^{96}Y and ^{96}Y to ^{96}Zr decays. This led to an intensity value for the 1750-keV gamma ray of 2.9(9) percent of the total decays of $^{96}\text{Y}^g$ and a value of 1.4(5) for the 1581-keV $E0$ transition. Our new decay scheme lead to a value of 4.8(9) percent of all $^{96}\text{Y}^g$ decays for the observed population of excited states in ^{96}Zr . Thus, the absolute beta feeding to the ground state of ^{96}Zr is 95.2(9) percent, in close agreement with the previous value¹⁵ of 95.0(15) percent, but very different from the value of 75% adopted in a recent data compilation for the $A=96$ chain.

III. LEVEL SCHEME OF ^{96}Zr

The levels of ^{96}Zr populated in the beta decay of $^{96}\text{Y}^g$ are shown in Fig. 8. This level scheme includes seven levels in addition to the 0_1^+ and 0_2^+ states which were the only levels reported^{1,15,21} previously as being populated by this decay. The placements of the γ rays in the decay scheme are based on the coincidence relations which are indicated by dots on the transition arrows. The beta decay half-life of 5.4(1) s is lower than the previously measured¹ value of 6.2(2) s. Several factors could have contributed to a higher value in the previous study. Howev-

er, the difference most probably lies in the fact that the source used in our study gave negligible direct production of $^{96}\text{Y}^m$ while ion sources used in earlier investigations gave a mixture of $^{96}\text{Y}^g$ and $^{96}\text{Y}^m$. The $\log f_0 t$ and $\log f_1 t$ values given in Fig. 8 were calculated using a Q_β value of 7140(40).²³

Spin and parity assignments for the three lowest-lying excited states in ^{96}Zr have been reported in a recent evaluation.¹ The levels at 1750 and 1897 keV are the first

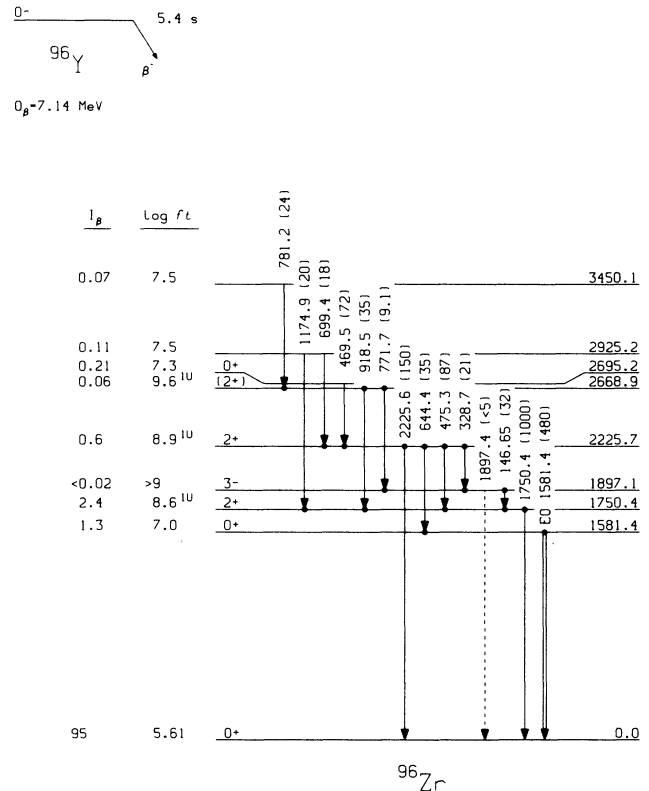


FIG. 8. Level scheme of $^{96}\text{Zr}_{56}$ as populated in the β^- decay of the 5.4-s 0^- ground state of ^{96}Y . The numbers in brackets above the transition arrows indicate relative transition intensities. For possible first-forbidden unique transitions, the $\log f_1 t$ values are indicated.

excited 2^+ associated with the 0^+ g.s. (Ref. 24) and the octupole (Ref. 25) excitations, respectively. The first excited level in ^{96}Zr has $J^\pi=0^+$ and decays to the ground state by an $E0$ transition.^{15,21} The coincidence of the 1581-keV $E0$ transition with the 644-keV γ ray necessitated the placement of this γ ray between the 2225-keV level and the 0_2^+ first excited state. An erroneous energy for the $E0$ transition reported in previous works²¹ was probably the reason that the 644-keV γ ray feeding the 0_2^+ level had been overlooked. The 2225-keV state has been found to have spin-parity 2^+ and has been interpreted as the 2^+ member of a band built on the first-excited 0^+ state.⁵ The angular correlation data for the 475–1750 keV $2_2^+ \rightarrow 2_1^+ \rightarrow 0_1^+$ cascade, in conjunction with the angular distribution results from the INS work,¹¹ indicate a very small (1%) $E2$ admixture for the 475-keV interband transition. In addition to the 0^+ 1581-keV and the 2^+ 2225-keV levels, a third member of the band has been recently suggested^{5,10} at 2857-keV with $J^\pi=4^+$, but we would not anticipate the population of this state in the low-spin β decay, and it is not observed.

The present angular correlation results confirm the previously made^{10,12} 0^+ spin-parity assignment for the 2694-keV level. The remaining three ^{96}Zr levels, which are populated with $\log ft$ values between 7 and 8, must also be of low spin. It is difficult, however, to make unambiguous spin assignments on these grounds alone. Nevertheless, the $\log f_1 t$ value of 9.6 is consistent with a spin and parity of 2^+ for the 2269-keV level, providing the β transition is unique first forbidden. Finally, we note that all of the states reported here are populated by the INS reaction^{5,11} and, with the exception of the 3450-keV level, have also been observed in a recent $(t, p\gamma)$ study.¹²

IV. DISCUSSION

A. The $0^- \rightarrow 0^+$ decay of $^{96}\text{Y}^g$ and double subshell closure

The 0^- assignment for the ^{96}Y GS was established in the previous work of Jung *et al.*^{8,9} Because this assignment is critical to our analysis of the ^{96}Zr levels, we briefly review the experimental evidence. The 932-keV level in ^{96}Y was found to be strongly populated with a $\log ft$ of 4.0 in the β decay of the 0^+ g.s. of ^{96}Sr , and thus a firm spin-parity assignment of 1^+ was made for the 932-keV state. The 932-keV level was shown to de-excite by an 809-keV transition which was in cascade with a 122-keV transition. The measured internal conversion coefficients of these transitions gave $E1$ and $M1(+E2)$ multipolarity for the 809- and 122-keV transitions, respectively. Jung *et al.*^{8,9} also performed angular correlation measurements for the 809–122 keV cascade, deduced a $1^+ \rightarrow 1^- \rightarrow 0^-$ sequence of levels, and thus established a spin-parity of 0^- for the ^{96}Y g.s.

The beta decay of the 0^- ^{96}Y g.s. to the 0^+ states of ^{96}Zr can shed light on the nature of ^{96}Zr . Our results confirm that beta decay mainly populates the ^{96}Zr g.s. with $\log ft$ of 5.6. This is one of the three fastest 0^- to 0^+ beta transitions now known.^{26,27} Such a fast first for-

bidden transition is characteristic for nuclei near doubly closed shells where the transitions involve states with nearly pure shell model configurations.²⁸ Thus, this class of transitions is of considerable interest because it can provide unique tests of β -decay theory, such as that discussed for ^{96}Zr and other cases by Khafizov.²⁹

There is considerable evidence to support the concept of a double subshell closure at ^{96}Zr . The energy of the first 2^+ state is high at 1750 keV and characteristic discontinuities are observed in the two-neutron and two-proton separation energies.²³ Furthermore, single-proton and single-neutron transfer reaction studies have shown^{2,30–32} that the $\pi(2p_{1/2})$ and $\nu(2d_{5/2})$ valence orbitals are almost filled, whereas the higher-lying orbitals do not contribute appreciably to the ground-state configuration. In particular, single proton stripping studies² have revealed an occupation probability of 0.91 for the $\pi(2p_{1/2})$ and $\pi(2p_{3/2})$ orbitals, and an occupation probability of only 0.05 for the $(1g_{9/2})$ proton orbital yielding almost pure, $91 \pm 3\%$, $\pi(2p_{1/2})^2$ configuration for the ^{96}Zr ground state wave function.

The significant hindrances of the beta feedings to the excited 0^+ states in ^{96}Zr , along with the enhancement of the β transition to the ground state, suggest that the configurations of these states are considerably different. At least for the 0_2^+ state the most natural choice is the $\pi(1g_{9/2})$ orbital which is the only valence proton orbital above $Z=40$ and below the $Z=50$ major shell closure. If we make the simplifying assumption that the $\pi(2p_{1/2})^2$ and $\pi(1g_{9/2})^2$ configurations are the main two proton configurations that contribute to the wave functions of the 0_1^+ and 0_2^+ states, respectively, then a simple two-level mixing formula can be applied:

$$|0_1^+\rangle = a |(2p_{1/2})^2 0^+\rangle + b |(1g_{9/2})^2 0^+\rangle, \quad (2a)$$

$$|0_2^+\rangle = -b |(2p_{1/2})^2 0^+\rangle + a |(1g_{9/2})^2 0^+\rangle, \quad (2b)$$

where $a^2 + b^2 = 1$. The $^{96}\text{Y}^g$ has been shown^{8,9} to have predominantly a $\pi(2p_{1/2})\nu(3s_{1/2})$ configuration. Since the β -decay matrix element connecting the odd $s_{1/2}$ neutron in $^{96}\text{Y}^g$ with a $p_{1/2}$ proton is much larger than for a $g_{9/2}$ proton, it is thus possible to determine the coefficients a and b from

$$ft(0_2^+)/ft(0_1^+) = a^2/b^2. \quad (3)$$

Using our measured ft values, we obtain almost pure ($a^2 = 96 \pm 2\%$) proton configurations of $(2p_{1/2})^2$ for the 0_1^+ ground state and of $(1g_{9/2})^2$ for the 0_2^+ state, respectively. Conversely, there is a small ($b^2 = 4 \pm 2\%$) admixture of the $2p_{1/2}$ configuration in the 0_2^+ state and (the same amount) of the $1g_{9/2}$ in the ground state of ^{96}Zr . Therefore, the ground state composition deduced from the beta decay is in quantitative agreement with the results of the single-proton transfer reaction studies.² The relative purity of the wave functions has already been suggested^{33,34} to account for the weakness of the $E0$ transition connecting the 0_1^+ and 0_2^+ states in ^{96}Zr , in contrast with ^{90}Zr .

Shell-model calculations³⁵ for ^{96}Zr have failed to reproduce the important feature of the double subshell

closure in ^{96}Zr , namely, the purity of its 0_1^+ and 0_2^+ states, despite the fact that these models can reproduce the general features and trends in the $^{90-96}\text{Zr}$ isotopes. One particular limitation of these models has been the severe restriction of the neutron space to include only the valence $2d_{5/2}$ and $3s_{1/2}$ orbitals, but not the important $\nu 1g_{7/2}$ orbital. Federman and Pittel³⁶ have shown the important influence of the occupation of the $\nu 1g_{7/2}$ orbital and the n-p interaction on the onset of deformation in the $A \sim 100$ region. In particular, they demonstrated that a collective 0_2^+ state can be produced by a mechanism which involves proton pairs and neutron pairs in the $\pi 1g_{9/2}$ and $\nu g_{7/2}$ spin partner orbitals. With a sufficient number of such pairs, a deformed state can indeed result. In the case of the excited 0^+ state in ^{96}Zr , a double subshell closure would prevent substantial occupation of the $\pi(1g_{9/2})$ and $\nu(1g_{7/2})$ orbits and, consequently, the 0_2^+ state is expected to be at most weakly deformed.

B. Deformation of the intruder band

Assuming that the 0_1^+ ground state and the 0_2^+ excited state are admixtures of spherical and deformed states which can be associated with the $(2p_{1/2})^2$ and $(1g_{9/2})^2$ proton configurations, respectively, one can write³⁷

$$|0_1^+\rangle = a |\text{sph}\rangle + b |\text{def}\rangle, \quad (4a)$$

$$|0_2^+\rangle = -b |\text{sph}\rangle + a |\text{def}\rangle, \quad (4b)$$

where a and b are the wave function amplitudes of (2). Hence the strength of the $E0$ transition between these 0^+ states is^{37,38}

$$\rho(E0) = abk\beta_2^2/eR_0^2, \quad (5)$$

where β_2 is the quadrupole deformation parameter characterizing the presumably deformed configuration and k is given by Bohr and Mottelson³⁸ as

$$k = (3/4\pi)ZeR_0^2[1 + (4\pi^2/3)(a_0/R_0)^2]. \quad (6)$$

The Woods-Saxon form factors,³⁹ $a_0 = 0.66$ fm and $R_0 = 5.54$ fm, yield $k/eR_0^2 = 11.4$ for ^{96}Zr . Using the amplitudes established from Eqs. (2) and (3), we have deduced the deformation parameter for the 0_2^+ level in ^{96}Zr . Its value, $\beta_2 = 0.20$, indicates a relatively small deformation for the excited 0^+ state but, nevertheless it is significantly larger than the value deduced⁴⁰ for the ground state ($\beta_2 = 0.081$).

Since we conclude that the intruder band is an independent set of excitations, we can deduce the collective parameters of the associated levels from the value of the β_2 parameter. A correlation of collective parameters has been established in a number of studies.⁴¹⁻⁴³ Figure 9 illustrates an empirical correlation of the energies of the first excited 2^+ levels and the energy ratios, E_{4^+}/E_{2^+} , plotted as a function of β_2 for the ground bands of nuclei in the $A \sim 96$ region. Using the value of $\beta_2 = 0.20$, one can deduce the energy of the 2^+ level to be approximately 600 keV above the 0_2^+ level and the energy ratio between the first 4^+ and 2^+ levels to be about

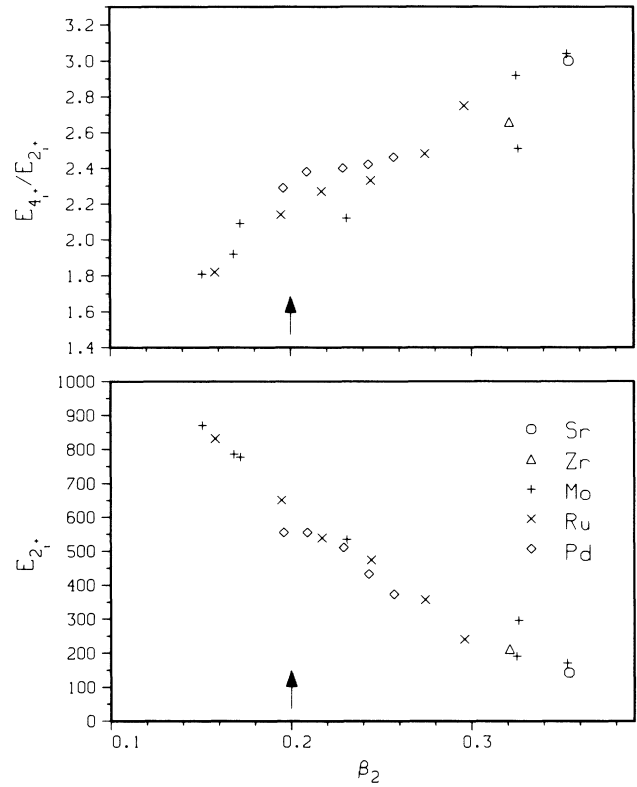


FIG. 9. Systematics of the energies of the 2_1^+ states and the energy ratios, $E_{4_1^+}/E_{2_1^+}$, as a function of the deformation parameter β_2 for even-even nuclei in the $A \sim 96$ region. Data are from Refs. 40 and 44. The value of $\beta_2 = 0.20$ derived for the 0_2^+ state of ^{96}Zr is indicated by an arrow.

2.2 (relative to the 0_2^+ bandhead energy). The 2^+ and 4^+ members of the 0_2^+ bands have been recently identified⁵ at 2225 keV and 2857 keV, respectively. Thus, the 2^+ level is 644 keV above the 0_2^+ state and the energy ratio is 2.0. The good agreement between the experimental and the predicted values must be a consequence of the weak mixing between these collective states and the corresponding levels of the ground state structure. Indeed, a strong $B(E2)$ branching ratio (100:0.7) in favor of the $2_2^+ \rightarrow 0_2^+$ transition over the $2_2^+ \rightarrow 0_1^+$ transition supports this weak mixing interpretation. It is also consistent with the small $\delta(E2/M1)$ mixing ratio deduced for the interband $2_2^+ \rightarrow 2_1^+$ transition. Furthermore, a beta transition from the 0^- ground state of ^{96}Y populates the 2_1^+ state by an unhindered⁴⁵ unique first-forbidden transition, thus confirming the small collectivity of the 2_1^+ level. The beta feeding to the 2_2^+ level is even smaller.

The collectivity of the band implies the simultaneous presence of valence protons and neutrons in the 0_2^+ state.³⁶ Casten⁴⁶ has recently shown that, for a given region like $A \sim 100$, there is a strong correlation between the structural properties and $N_p N_n$, the product of the number of valence neutrons and protons. This correlation implies⁴⁷ that nuclei which belong to the same region and have similar collective properties, must also

have a similar product number of the valence particles. Such intercomparison has been long expected^{48,49} to include also the intruder bands. Indeed, in a recent study of ⁹⁸Zr, Meyer *et al.*⁶ have identified eight excited states of the intruder ⁹⁸Zr* band and have demonstrated a correspondence with the levels in the even-even ¹⁰²Ru nucleus. We expect to find a similar correspondence for ⁹⁶Zr*, with the exception that, unlike ⁹⁸Zr where the coexisting structures are strongly mixed,⁶ one can be more specific about the number of valence particles for the almost pure ⁹⁶Zr* intruder band. Figure 10 illustrates the systematics of the energies of the first excited 2⁺ states and the energy ratios plotted against the neutron number for ⁴²Mo, ⁴⁴Ru, and ⁴⁶Pd nuclei, where the valence proton orbital is 1g_{9/2}, as it is also for the 0₂⁺ level in ⁹⁶Zr. The Cd nuclei are not included since their structures are influenced^{49,50} by configurations intruding across the Z=50 shell gap. The neutron space has been arbitrarily limited to 52 ≤ N ≤ 64. As indicated in the figure, only two nuclei in this region, namely ⁹⁸Ru₅₄ and ¹⁰⁰Pd₅₄, match both the experimental energy, E₂₊ = 644 keV, and the energy ratio of 2.0. Furthermore, the value of β₂ = 0.195(3) measured⁴⁵ for ⁹⁸Ru is identical to the value of 0.20 deduced for the ⁹⁶Zr* band. Both ⁹⁸Ru and ¹⁰⁰Pd are at N=54, and thus have four neutrons above the N=50 shell; ⁹⁸Ru has four protons above the Z=40 shell, while ¹⁰⁰Pd has four-proton holes below the

Z=50 shell. This close correspondence implies that the ⁹⁶Zr* intruder bandhead has effectively four valence neutrons and four protons.

In order to estimate independently the number of valence particles in the 0₂⁺ state in ⁹⁶Zr, one has to establish the nearest shell closure. In the case of a second ground state in a doubly closed subshell nucleus the task is rather simple. A disruption of either of the subshell gaps would greatly increase the number of valence particles and would result in a large β₂. However, the deformation parameter deduced for the excited 0₂⁺ state, β₂ = 0.2, indicates that the counting of valence particles for this state must be also limited by the shell gaps at Z=40 and N=56. On the other hand, the value of β₂ is sufficiently large (see Fig. 9) to verify through the n-p interaction a simultaneous presence of valence protons and neutrons. Thus the simultaneous promotion of one proton pair and one neutron pair across the Z=40 and N=56 shell gaps is implied. By treating particles and holes above and below the closed shell equally, one arrives with four valence protons and four valence neutrons for the 0₂⁺ state in agreement with the numbers implied from the correspondence of the ⁹⁶Zr* to ⁹⁸Ru and ¹⁰⁰Pd. It is not clear to which valence orbital the neutron pair is promoted, although the most likely solution may involve a combination of a few orbitals. However, in the view of the occupation of the proton (1g_{9/2})² orbital, some occupation of the neutron 1g_{7/2} orbital is almost certain due to the strong attractive n-p interaction in those orbitals.³⁶ These ideas complement earlier work⁵ in which the 4p-4h configuration for the 0₂⁺ state in ⁹⁶Zr has been also proposed on a different basis, using multiparticle transfer data.⁵¹

V. SUMMARY

The beta decay of the 0⁻ ⁹⁶Y isomer was found to populate several excited states in ⁹⁶Zr. The unhindered first-forbidden transitions to the 0⁺ ground state and the first 2⁺ level provide additional arguments in favor of a double subshell closure at Z=40, N=56. A large hindrance of the beta decay to the 0₂⁺ state has been measured indicating a structure completely different from that of the ground state. A small mixing of the π(2p_{1/2})² configuration was deduced for the otherwise pure (1g_{9/2})² proton configuration of the 0₂⁺ state. Also, a deformation parameter of 0.20 was obtained for the 0₂⁺ level through the E0 transition strength. From the systematics of the collective variables in the A ~ 96 region one expects the E₂₊ ~ 600 keV and the energy ratio E₄₊/E₂₊ ~ 2.2 corresponding to this β₂. These predictions closely match the values of 644-keV and the energy ratio of 2.0 determined for the collective band in ⁹⁶Zr*. Furthermore, all evidence indicates that the mixing of the GS and intruder bandhead is very weak. Consistent with the previous findings⁶ on ⁹⁶Zr*, we find a correspondence between the vibrational-like band in ⁹⁶Zr* and the lowest states of ⁹⁸Ru (Z=40+4, N=50+4) and ¹⁰⁰Pd (Z=50-4, N=50+4). This correspondence implies similar effective occupation of the valence proton and neutron orbitals and thus sup-

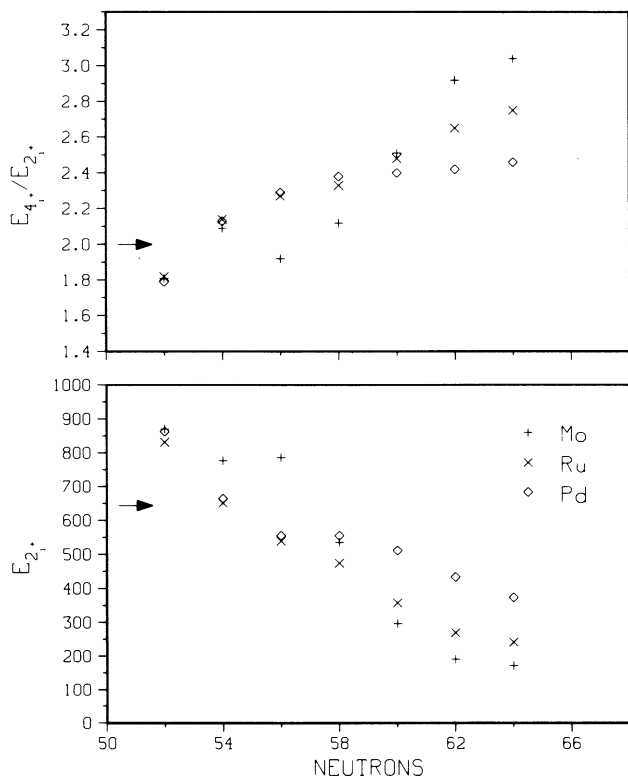


FIG. 10. Energies of the 2₁⁺ levels and energy ratios, E₄₊/E₂₊, as a function of the neutron number for Mo, Ru, and Pd nuclei with 52 ≤ N ≤ 64. Data are from Sakai (Ref. 44). The values found for the coexisting band in ⁹⁶Zr* are indicated by arrows.

ports the concept⁵ that the O_2^+ state of ^{96}Zr contains a substantial four-particle, four-hole component.

ACKNOWLEDGMENTS

The authors would like to thank R. F. Casten for the many valuable discussions and comments. Furthermore, stimulating discussions with E. A. Henry, K. Heyde, R.

U. Khafizov, J. van Klinken, J. D. Robertson, R. Siemssen, and K. Sistemich are also gratefully acknowledged. This research has been performed in part under contracts Nos. DE-AC02-79ER10493, DE-AS05-79ER10494, DE-AC02-76CH00016, and W-7405-ENG-48 with the U.S. Department of Energy and National Science Foundation Grant No. INT-8512479.

*Permanent address: Institute of Isotopes, Budapest, H-1525, Hungary.

†Present address: Lawrence Livermore National Laboratory, Livermore, CA 94550.

¹H.-W. Mueller, Nucl. Data Sheets **35**, 281 (1982).

²M. R. Cates, J. B. Ball, and E. Newman, Phys. Rev. **187**, 1682 (1969).

³E. R. Flynn, J. G. Beery, and A. G. Blair, Nucl. Phys. **A218**, 285 (1974).

⁴A. Saha, G. D. Jones, L. W. Put, and R. H. Siemssen, Phys. Lett. **82B**, 208 (1979).

⁵G. Molnár, S. W. Yates, and R. A. Meyer, Phys. Rev. C **33**, 1843 (1986).

⁶R. A. Meyer, E. A. Henry, L. G. Mann, and K. Heyde, Phys. Lett. **177B**, 271 (1986).

⁷G. Lhersonneau, D. Weiler, P. Kohl, H. Ohm, K. Sistemich, and R. A. Meyer, Z. Phys. A **323**, 59 (1986).

⁸G. Jung, B. Pfeiffer, P. Hungerford, S. M. Scott, F. Schussler, E. Monnard, J. A. Pinston, L. J. Alquist, H. Wollnik, and W. D. Hamilton, Nucl. Phys. **A352**, 1 (1981).

⁹G. Jung, Ph.D. thesis, Universität Giessen, 1980.

¹⁰G. Molnár, S. W. Yates, E. W. Kleppinger, T. Belgya, B. Fazekas, A. Veres, and R. A. Meyer, in *Symmetries and Nuclear Structure*, edited by R. A. Meyer and V. Paar (Harwood, New York, 1987), p. 237.

¹¹G. Molnár, S. W. Yates, E. W. Kleppinger, T. Belgya, B. Fazekas, and A. Veres (unpublished).

¹²E. A. Henry, in *Nuclear Structure, Reactions, and Symmetries*, edited by R. A. Meyer and V. Paar (World-Scientific, Singapore, 1986), p. 616.

¹³E. A. Henry, R. J. Estep, R. A. Meyer, J. Kantele, D. J. Decman, L. G. Mann, R. K. Sheline, W. Stöfl, and L. E. Ussery, in *Recent Advances in the Study of Nuclei Off the Line of Stability*, Vol. 324 of the *ACS Symposium Series*, edited by R. A. Meyer and D. S. Brenner (ACS, Washington, D.C., 1986), p. 190.

¹⁴M. Shmid, R. L. Gill, and C. Chung, Nucl. Instrum. Methods **211**, 287 (1983).

¹⁵G. Sadler, T. A. Khan, K. Sistemich, J. W. Grüter, H. Lawin, W. D. Lauppe, H. A. Selić, M. Shaanan, F. Schussler, J. Blachot, E. Monnard, G. Bailleul, J. P. Bocquet, B. Pfeiffer, H. Schrader, and B. Fogelberg, Nucl. Phys. **A252**, 365 (1975).

¹⁶A. Wolf, C. Chung, W. B. Walters, G. Peaslee, R. L. Gill, M. Shmid, V. Manzella, M. L. Stelts, H. I. Liou, R. E. Chrien, and D. S. Brenner, Nucl. Instrum. Methods **206**, 397 (1983).

¹⁷D. C. Camp and A. L. Van Lehn, Nucl. Instrum. Methods **76**, 192 (1969); **87**, 147 (1970).

¹⁸S. M. Scott, W. D. Hamilton, P. Hungerford, D. D. Warner, G. Jung, and K. D. Wunsch, J. Phys. G **6**, 1291 (1980).

¹⁹D. W. O. Rogers, Nucl. Instrum. Methods **127**, 253 (1975).

²⁰J. van Klinken, J. F. W. Jansen, W. Z. Venema, and B. Pfeiffer, in *Nuclear Structure, Reactions, and Symmetries*, edited by R. A. Meyer and V. Paar (World-Scientific, Singa-

pore, 1986), p. 665.

²¹T. A. Khan, W. D. Lauppe, H. A. Selić, H. Lawin, G. Sadler, M. Shaanan, and K. Sistemich, Z. Phys. A **275**, 289 (1975).

²²J. van Klinken (private communication).

²³A. H. Wapstra and G. Audi, Nucl. Phys. **A432**, 1 (1985).

²⁴Y. P. Gangrskii and I. K. Lemberg, Yad. Fiz. **1**, 1025 (1965) [Sov. J. Nucl. Phys. **1**, 731 (1965)].

²⁵E. R. Flynn, D. D. Armstrong, and J. G. Beery, Phys. Rev. C **1**, 703 (1970).

²⁶C. A. Galiardi, G. T. Garvey, and J. R. Wroubel, Phys. Rev. C **28**, 2423 (1983).

²⁷M. P. Webb, Nucl. Data Sheets **26**, 145 (1979).

²⁸J. Damgaard, R. Broglia, and C. Riedel, Nucl. Phys. **A135**, 310 (1969).

²⁹R. U. Khafizov, Phys. Lett. **162B**, 21 (1985).

³⁰B. M. Preedom, E. Newman, and J. C. Hiebert, Phys. Rev. **166**, 1156 (1968).

³¹B. L. Cohen and O. V. Chubinsky, Phys. Rev. **131**, 2184 (1963).

³²M. M. Stautberg, R. R. Johnson, J. J. Kraushaar, and B. W. Ridley, Nucl. Phys. **A104**, 67 (1987).

³³R. Julin, J. Kantele, M. Luontama, and A. Passoja, Z. Phys. A **303**, 147 (1981).

³⁴D. Burch, P. Russo, H. Swanson, and E. G. Adelberger, Phys. Lett. **40B**, 357 (1972).

³⁵D. H. Gloeckner, Nucl. Phys. **A253**, 301 (1975).

³⁶P. Federman and S. Pittel, Phys. Rev. C **20**, 820 (1979).

³⁷J. Kantele, R. Julin, M. Luontama, A. Passoja, T. Poikolainen, A. Bäcklin, and N.-G. Jonsson, Z. Phys. A **289**, 157 (1979).

³⁸A. Bohr and B. R. Mottelson, *Nuclear Structure* (Benjamin, Reading, Mass., 1975), Vol. 2, p. 358.

³⁹A. B. Smith, P. Guenther, and J. Whalen, Nucl. Phys. **A244**, 213 (1975).

⁴⁰S. Raman, C. H. Malarkey, W. T. Milner, C. W. Nestor, Jr., and P. H. Stelson, At. Data Nucl. Data Tables **36**, 1 (1987).

⁴¹L. Grodzins, Phys. Lett. **2**, 88 (1962).

⁴²M. A. J. Mariscotti, G. Scharff-Goldhaber, and B. Buck, Phys. Rev. **178**, 1864 (1969).

⁴³A. Goldhaber and G. Scharff-Goldhaber, Phys. Rev. **17**, 1171 (1978).

⁴⁴M. Sakai, At. Data Nucl. Data Tables **31**, 399 (1984).

⁴⁵S. Raman and N. B. Grove, Phys. Rev. C **7**, 1995 (1973).

⁴⁶R. F. Casten, Phys. Lett. **152B**, 145 (1985).

⁴⁷R. F. Casten, Phys. Rev. C **33**, 1819 (1986).

⁴⁸K. Heyde, P. Van Isacker, J. Moreau, and M. Waroquier, in *In-Beam Nuclear Spectroscopy*, edited by Zs. Dombrádi and T. Fényes (Akadémiai Kiadó, Budapest, 1984), p. 151.

⁴⁹A. Aprahamian, D. S. Brenner, R. F. Casten, R. L. Gill, A. Piotrowski, and K. Heyde, Phys. Lett. **140B**, 22 (1984).

⁵⁰K. Heyde, P. Van Isacker, M. Waroquier, J. L. Wood, and R. A. Meyer, Phys. Rep. **102**, 291 (1983).

⁵¹A. M. Van den Berg, A. Saha, G. D. Jones, L. W. Put, and R. H. Siemssen, Nucl. Phys. **A429**, 1 (1984).